Applied Radiation and Isotopes 235 (2026) 112674

Contents lists available at ScienceDirect

Applied Radiation and Isotopes

journal homepage: www.elsevier.com/locate/apradiso

Standardization of ^{243}Am

M.R. Bodine *, L. Laureano-Pérez, R. Collé, J. Wilde, R. Fitzgerald, L. Pibida, J. La Rosa, A.J. Pearce, R. Essex, D.E. Bergeron, M. Carlson

Physical Measurement Laboratory, National Institute of Standards and Technology (NIST), Gaithersburg, MD, 20899, United States

ARTICLE INFO

Keywords:
Anticoincidence
Americium-243
CNET
TDCR
Gamma-ray spectrometry
DES
Liquid scintillation
LTAC
Mass spectrometry

ABSTRACT

Americium's longest-lived isotope, americium-243, has a half-life of 7367(23) years. It decays into neptunium-239 through alpha decay. Americium has a few practical uses: as a monitor for radioactive contamination and as a tracer for radiochemical processes. An ^{243}Am solution was standardized by 4παβ liquid scintillation (LS) spectrometry with two commercial LS counters. The beta detection efficiencies for the ^{243}Am daughter (^{239}Np) were calculated for the CIEMAT/NIST efficiency tracing (CNET) and the triple-to-double coincidence ratio (TDCR) methods using a modified MICELLE2 code and accounting for contributions from the delayed ($T_{1/2} = 193$ ns) γ-ray emission from an excited state of ^{239}Pu. Five confirmatory measurements of the activity were performed by 1) LS counting comparative measurements against the previous version of this Standard Reference Material (SRM) 4332e, which was standardized in 2008 by CIEMAT/NIST efficiency tracing using ^{3}H as the detection efficiency monitor; 2) live-timed anticoincidence (LTAC) measurements; 3) triple-to-double coincidence ratio counting; 4) gamma spectrometry with high resolution HPGe detectors; and 5) decay energy spectrometry (DES) using transition edge sensors (TES). Alpha spectrometry measurement results gave a combined activity of ^{239,240}Pu of 0.087(2) Bq·g^{-1}. The activity ratio of ^{241}Am/^{243}Am was obtained by alpha spectrometry, gamma-ray spectrometry, mass spectrometry, and DES, with an average value of 0.00168(3). Mass spectrometry was also used to obtain values for ^{239}Pu, ^{240}Pu and ^{241}Pu impurities.

1. Introduction

Americium-243 is the longest-lived americium isotope; however, it is not found in nature. It is formed in the nuclear fuel cycle by neutron capture of ^{242}Pu followed by beta decay. Accurate standardization of ^{243}Am is needed as a tracer for the measurements of ^{241}Am content in environmental samples. Americium-243 is also used as a calibration source for gamma-ray spectrometry.

Americium-243 has a half-life of 7367 (23) a (Bé et al., 2010, Decay Data Evaluation Project, 2025) and decays by alpha decay to the ground and excited states of ^{239}Np (Bé et al., 2008) There is also the decay path of a minute branch of 3.8(7) 10^{-9} % by spontaneous fission. Neptunium-239 has a half-life of 2.356(3) d, and decays by beta emission to ^{239}Pu. Both decays feed numerous gamma transitions. Due to the short half-life of ^{239}Np, ^{243}Am will typically be encountered in radioactive equilibrium with its daughter.

Americium-243 standards have been issued by the National Institute of Standards and Technology (NIST) starting in 1974, with different series being derived from different stock materials. The previous issues of standard reference materials (SRMs) include SRM 4332 in 1974, SRM 4332b in 1984, SRM 4332c in 1990, SRM 4332d in 2005, and SRM 4332e in 2008. The most recent version, SRM 4332e (NIST, 2019) was prepared from Eckert & Ziegler Isotope Products[1] source no. 1292-42. A total of 232 ampoules were produced, with the remainder of the source solution set aside for future production and measurement.

This paper describes the series of measurements that ultimately support the issue of an ^{243}Am solution, SRM 4332f. In addition to 4παβ liquid scintillation (LS) counting with ^{3}H efficiency tracing, which was used in the past ^{243}Am SRM characterizations, we describe confirmatory primary massic activity measurements by live-timed anticoincidence counting (LTAC), gamma-ray spectrometry, triple-to-double coincidence ratio (TDCR) LS counting, and decay energy spectrometry (DES).

This article is part of a special issue entitled: ICRM 2025 published in Applied Radiation and Isotopes.

* Corresponding author.
E-mail address: madeleine.bodine@nist.gov (M.R. Bodine).

[1] Certain commercial equipment, instruments, or materials are identified in this paper to foster understanding. Such identification does not imply recommendation by the National Institute of Standards and Technology, nor does it imply that the materials or equipment identified are necessarily the best available for the purpose.

https://doi.org/10.1016/j.apradiso.2026.112674
Received 31 July 2025; Received in revised form 9 March 2026; Accepted 23 April 2026
Available online 2 May 2026

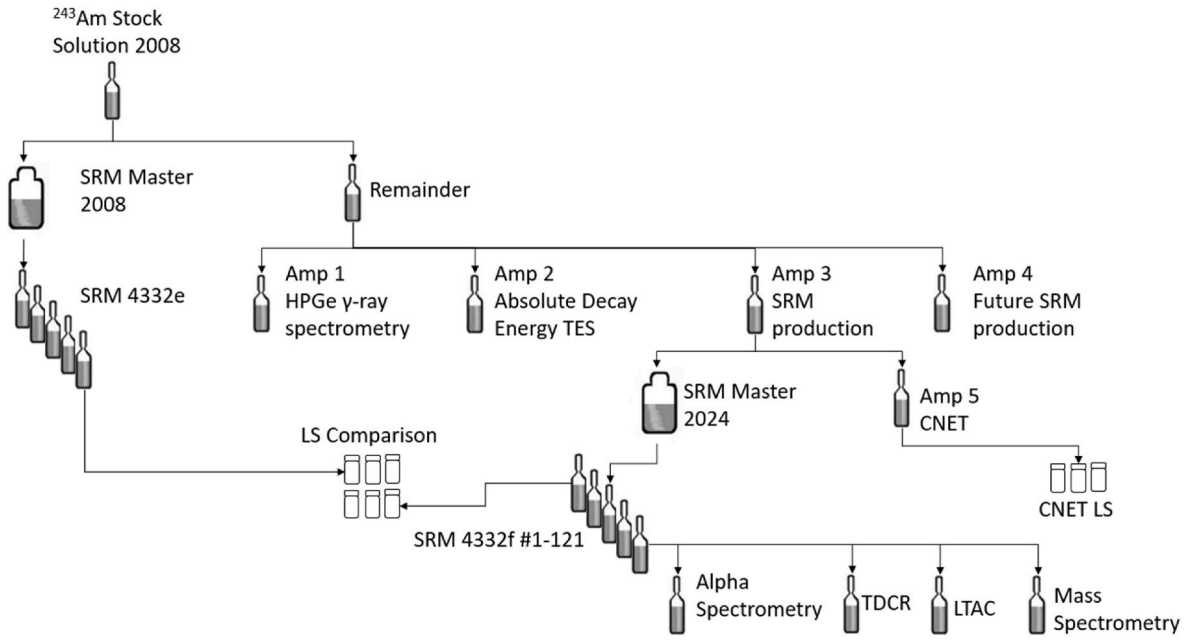

Fig. 1. Scheme for the dilutions and source preparation for ^{243}Am as used for calibration and confirmatory measurements.

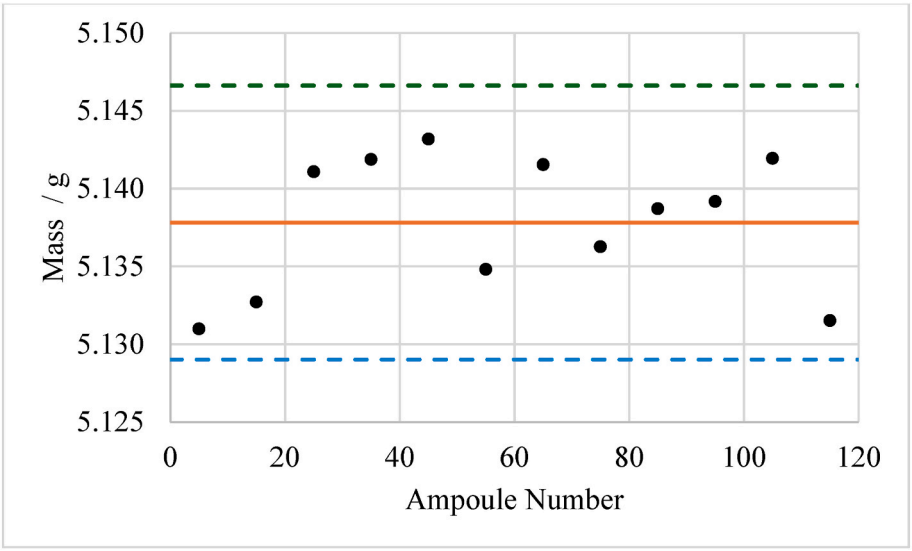

Fig. 2. Dispensed masses of the SRM 4332f dispensing solution *m* in units of grams in 5 mL aliquants as a function of filling order. The solid horizontal line corresponds to mean mass = 5.1378 g and the dashed lines represent the upper and lower limits for the ± 2*s* about the mean where *s* = 0.0044 g is the standard deviation for the distribution of 12 samples.

We discuss improvements to the LS efficiency models and present characterizations of the radionuclidic impurities by multiple methods, including alpha spectrometry, DES, and mass spectrometry.

2. Experimental methods, results and discussion

2.1. Overview

The scheme used to prepare the ^{243}Am standard and the counting and confirmatory measurement sources are shown in Fig. 1. The stock solution used to prepare both SRM 4332e and SRM 4332f are linked through gravimetrically determined dilution factors (Campion, 1975; Sibbens and Altzitzoglou, 2007). The certified ^{243}Am massic activity for the standards was obtained from a primary standardization based on 4παβ liquid scintillation (LS) spectrometry, with corrections for several impurities and for the ^{239}Np daughter, by using the CIEMAT/NIST efficiency tracing method (CNET[2])(Collé and Zimmerman, 1997; Barresi et al., 2022; Broda et al., 2007; Coursey et al., 1986; Laureano-Perez et al., 2007; Zimmerman and Collé, 1997). A direct LS comparison of the SRM 4332f was made with the previous dissemination SRM 4332e. All aliquots of the LS counting sources were linked to the dispensing solutions by gravimetric determinations.

[2] The acronym CNET refers to the CIEMAT/NIST Efficiency Tracing method. CIEMAT/NIST refers to the two laboratories that collaborated in developing the protocol for this LS tracing methodology, i.e., the Centro de Investigaciones Energéticas, Medioambientales y Tecnológicas (CIEMAT) and the National Institute of Standards and Technology (NIST).

2.2. Preparation of primary solution and SRM ampoules

To prepare the primary solution for SRM 4332f, the stock solution remainder from 2008 was first diluted into four ampoules, #1 for HPGe, #2 for DES, #3 for SRM production, #4 for future SRM production. Ampoule #3 was diluted with 1.018 mol L^{-1} HNO_3, using a dilution factor (DF) of 398.28 (8), becoming SRM Master 2024.

The SRM 4332f Master 2024 solution was dispensed into 120 borosilicate glass ampoules using a Microlab 620 single-syringe automatic dispenser (Hamilton Company, Reno, NV, USA). The ampoules used are designated as NIST-3 ampoules (Collé, 2019). The solution consisted of 1.02(3) mol · L^{-1} HNO_3 with a density of 1.032(2) g · mL^{-1} at 22 °C. Twelve ampoules, roughly every tenth ampoule, were weighed before and after filling to obtain an estimate of the dispensing precision and contained mass. Weighing was performed with an electronic analytical balance (Mettler AE240). The average mass was 5.1378 g with a relative standard deviation of 0.086 % for the 12 samples. The data were tested and found to fit a normal distribution. Fig. 2 shows the relative invariance of the solution mass with sample filling order.

3. Measurement methods

3.1. Liquid scintillation counting efficiencies

For ^{239}Np, LS efficiencies for TDCR and CNET were calculated using a modified version of the MICELLE2 code (Kossert and Grau Carles, 2010) and a simplified decay scheme that included thirteen β-γ cascades (with up to four γ transitions per cascade) with probability >1 %, accounting for 99.7 % of all decays (Bé et al., 2008). The branch weights were renormalized to distribute the remaining 0.3 % of decays to the cascades closest in energy. The major beta transitions for ^{239}Np are all "allowed" except for the β(0,8) transition which is 1st forbidden. The MICELLE2 code was modified to read the beta spectra directly from the BetaShape v. 2.2 output available from the Decay Data Evaluation Project (DDEP) (Mougeot, 2015a, 2015b, 2017). The code was also modified to output single photomultiplier tube (PMT) efficiencies (following Kossert et al., 2014), which were important for corrections associated with the long-lived 8th excited state of ^{239}Pu.

In the simplified ^{239}Np decay scheme, 38.9(9) % of β decays feed the 8th excited state of ^{239}Pu (β(0,8), see Table S1); this state is long-lived ($T_{1/2}$ = 193 ns; Bé et al., 2008; Barresi et al., 2022) compared to the coincidence resolving time used in the TDCR measurements (τ_R = 60 ns).

The efficiency calculations for decays involving β(0,8) must consider the following cases:

1. Relaxation from the excited state takes place with a delay less than τ_R after the β(0,8) emission. In this case, from the perspective of the TDCR electronics, the scintillation events from the two decays effectively occur simultaneously. Thus, we treat the β(0,8)+γ8 decays as a single cascade in MICELLE2, with doubles efficiency, $\varepsilon_{D,\beta 8\gamma 8}$. This is the $(1 - P_s)$ term in Equation (1), where $\varepsilon_{D,\beta 8\gamma 8}$ accounts for doubles events resulting from the beta, the gamma or a combination (1 PMT hit due to beta, 1 PMT hit due to gamma).
2. Relaxation from the excited state takes place with a delay greater than τ_R after the β(0,8) decay. This is the P_s term in Equation (1), which itself contains two terms:
   a. If the β(0,8) decay is detected, the doubles counting efficiency, $\varepsilon_{D,\beta 8}$, is calculated by MICELLE2 for the beta-transition only. The dead-time from the β would veto any subsequent signal from the γ-ray.
   b. Alternatively, if no PMTs are triggered by the β(0,8) decay, with probability $(1 - \varepsilon_{S,\beta 8})$, the γ-ray emission is treated as an independent decay, with doubles efficiency $\varepsilon_{D,\gamma 8}$ calculated by MICELLE2 for the gamma-transitions only.

The total logical sum of doubles efficiency for the β(0,8) decays is calculated as

$$\varepsilon_{D,8} = (1 - P_s)\varepsilon_{D,\beta 8\gamma 8} + P_s\left[\varepsilon_{D,\beta 8} + (1 - \varepsilon_{S,\beta 8})\varepsilon_{D,\gamma 8}\right] \quad (1)$$

where P_s is the probability that the relaxation from the 8th excited state occurs after τ_R,

$$P_s = e^{-\ln(2)\left(\tau_R / T_{1/2(\gamma)}\right)} \quad (2)$$

Importantly, all the γ8 decays are accounted for once, and only once, in Equation (1). The $(1 - P_s)$ term accounts for the case when the γ8 is coincident with β(0,8), and the second P_s term accounts for the case when they are not coincident (γ delayed by more than τ_R).

The total triples efficiency for the β(0,8) decays is similarly calculated. Logical sum of doubles and triples efficiencies from all ^{239}Np cascades are weighted and combined in Microsoft Excel. The ^{243}Am counting efficiency ($\varepsilon_{D,Am-243}$) is estimated as 1.

The massic activity of ^{243}Am can be expressed in terms of the logical sum of doubles count rate corrected for background and accidental coincidences (Dutsov et al., 2020), (R_D^+), as

$$A_m = \frac{R_D^+}{\varepsilon_D^+ m} \quad (3)$$

where

$$\varepsilon_D^+ = \varepsilon_{D,Am-243} + \sum_i f_i \varepsilon_{D,i} \quad (4)$$

and f_i is the impurity fraction (A_i/A_{Am-243}) for the ith impurity (to include ^{239}Np), $\varepsilon_{D,i}$ is the estimated logical sum of doubles counting efficiency for the ith impurity, and m is the mass of solution added to the LS source.

CNET corrections for the delayed γ-ray emission associated with β(0,8) decays are somewhat simpler. For the PerkinElmer Tri-Carb 4910 TR (PerkinElmer, Waltham, MA), τ_R is user-defined and was set to 18 ns in these studies. The short resolving time results in few γ-ray emissions before the resolving time expires ($1 - P_s = 0.063$). The counting efficiencies are therefore dominated by the first (β-only) term. The massic activity of ^{243}Am is determined from equations (3) and (4) using the measured count rates and CNET efficiencies.

For direct comparison with SRM4332e, CNET efficiencies were also calculated using the CN2003 code (Günther, 2003), due to it being used during the previous productions of SRMs. The beta spectrum calculations were unaltered from the original code and these calculations did not account for the delayed γ-ray emission associated with β(0,8) decays. Previous experimental work for Pu-241 SRM 4340b was used to estimate the doubles counting efficiency (NIST, 2008).

3.2. CNET and 4παβ liquid scintillation counting

The certified massic activity of SRM 4332f was determined by 4παβ liquid scintillation (LS) counting using the CNET method and using the MICELLE2 code for the β-efficiencies of ^{239}Np. The reference date used for all measurements was 1200 EST, 08 March 2024. Two different instruments were used for this set of LS measurements (i) PerkinElmer Tri-Carb 4910 TR I (PerkinElmer, Waltham, MA) and (ii) Beckman LS 6500 (Beckman Coulter, Fullerton, CA). These two counters have considerably different operation conditions characteristics (detection threshold, photomultiplier efficiency, deadtime, amplification, signal conversion.) Using two counters helps to ensure variation in measurement conditions during standardization, allowing results to be independent from instrument characteristics.

In all cases, sources were prepared gravimetrically in 20 mL glass LS vials with Ultima Gold AB (UGAB) scintillation fluid (PerkinElmer, Waltham, MA). Due to the low level of activity in the SRM ampoules, the CNET sources were prepared with the remainder of ampoule #3 that

Table 1
Cocktail Series, where N_s = number of samples in each series, M = mass of scintillation fluid in each cocktail (in grams), and f_w = aqueous mass fraction in cocktail.

Cocktail series	Scintillant	N_s	M/g	f_w	*Solution(s)*
I	UGAB	6	9.8	0.07	4332f – 27
II	UGAB	6	9.8	0.07	4332f – 115
III	UGAB	6	9.8	0.07	4332e – 67
IV	HF	5	9.7	0.07	4332f – 62
V	HF	5	9.7	0.07	4332f – 93
VI	HF	5	9.7	0.07	4332e – 229
VII	UGAB	6	9.8	0.06	^{243}Am Stock Dilution
VIII	UGAB	6	9.8	0.06	4927g Dilution

was used to prepare the SRM Primary solution, which is gravimetrically linked to the SRM ampoules. Six ^{243}Am sources and five ^{3}H (NIST, 2015) sources were prepared; the sources were matched by composition and quench and were quenched using nitromethane. Each source was counted for 10 min, for 5 cycles, on each of the two counters, for two runs.

The calculated massic activity without impurity correction and accounting for the ^{239}Np daughter in equilibrium for SRM4332f was 48.51 (12) Bq · g^{-1}. All data were subjected to normality testing, with combinations of the variables counter and run, as well as a combined test of all LS measurements. The Anderson-Darling and Wilk-Shapiro normality tests for all sets of data passed at 95% confidence.

3.3. Triple-to-double coincidence ratio (TDCR) counting

Sources were prepared gravimetrically in 20 mL glass LS vials with Ultima Gold AB (UGAB) scintillation fluid (PerkinElmer, Waltham, MA). On the NIST TDCR counter (Zimmerman et al., 2004), sources were measured with a coincidence resolving time of 60 ns and the extendable deadtime was set to 50 μs. Source and blank count rates were corrected for accidental coincidences (Dutsov et al., 2020). Each time a source was inserted into the chamber, it was counted for three repeats of 1 h, resulting in approximately $2.5{\cdot}10^5$ to $3{\cdot}10^5$ net counts in the logical sum of doubles (LSD) channel for each repeat. Each source was inserted three times with no gray filter and a subset were also counted with gray filters to vary the counting efficiency.

The calculated massic activity for SRM 4332f from TDCR was 48.45 (15) Bq · g^{-1}. All data were subjected to normality testing, with combinations of the variables source, filter and run, as well as a combined test of all TDCR measurements.

3.4. LS-based comparison

LS comparative measurements were made between SRM 4332f and SRM4332e. These two sets of comparisons of the previous SRM to the new version are facilitated by the gravimetric link of the solutions, and function as a check on the activity determination of the new SRM.

The two scintillants used were Ultima Gold AB (UGAB) and Hionic-Fluor (HF) (PerkinElmer, Waltham, MA). The sources were prepared from several SRM ampoules, and the cocktail series are given in Table 1. The series used in this experiment are I – VI. The sources were measured two times on each of two counters, TriCarb and Beckman. Each measurement consisted of three cycles of 60-min counts. The massic activity ratio of 4332f to 4332e was found to be 1.2535(25), where the stated uncertainty was calculated from the standard deviation of repeat determinations only. All data were subjected to normality testing, with combinations of the variables scintillant, counter, and run, as well as a combined test of all LS measurements for each of the new and old SRM solutions. The normality tests all passed at 95% confidence.

Sources from series I, II, and III in Table 1 were also measured on the NIST triple-to-double coincidence ratio (TDCR) LS counter (Zimmerman et al., 2004). The sources were measured with a coincidence resolving time of 60 ns and the extendable deadtime was set to 50 μs. Source and blank count rates were corrected for accidental coincidences (Dutsov et al., 2020). Each source was inserted three times with no gray filter, and a subset was also counted with gray filters to vary the counting efficiency. The massic LSD count rates were compared, giving a ratio between 4332f to 4332e of 1.2528(30), where the stated uncertainty is calculated from the standard deviation of repeat determinations only.

3.5. Impurity analyses

3.5.1. Alpha spectrometry

Alpha spectrometry was used to investigate the potential impact and activity of the impurities ^{241}Am and ^{239}Pu. To investigate ^{241}Am, four identical solid sources were prepared from the remainder ampoule of the LS comparison sources, expressed in terms of activity as $f_{\mathrm{Am-241}} = \frac{A_{\mathrm{Am-241}}}{A_{\mathrm{Am-243}}}$. The samples were prepared by electrodeposition onto stainless steel disks from solutions composed of 0.1 g SRM 4332f dissolved in a sodium hydrogen sulfate-sodium sulfate buffer ($NaHSO_4/Na_2SO_4$ mole ratio = 0.197; pH = 2.7). The $f_{\mathrm{Am-241}}$ was determined to be 0.00162 (19), where the uncertainty is the combined standard uncertainty, where counting statistics and within and between uncertainties of replicates were considered.

To investigate ^{239}Pu, radiochemical separation of the Pu impurity was required to remove interferences from ^{241}Am fraction in the samples. To do this, four sources were made using an aliquot of approximately 1 g of SRM 4332f and 0.3 g of ^{242}Pu spike from a dilution of SRM 4334h (NIST, 2005) (0.282 Bq·g^{-1}) as a tracer. For each sample, the volume was brought to approximately 4 mL with 0.7 mL deionized H_2O and 2 mL of 1 mol L^{-1} HNO_3. 50 mg of $(NH_4)_2Fe(SO_4)_2$ was added to each, followed by 0.5 mL of a 25 % mass fraction $NaNO_2$ solution. The solutions were then brought to 6 mL with the addition of 0.5 mL of DI H_2O and 1 mL concentrated HNO_3, giving a final HNO_3 concentration of approximately 3 mol L^{-1}. The solutions were loaded onto TEVA resin (TEtraValents Actinides resin, Eichrom, Inc., Lisle, IL, USA) columns, and the TEVA columns rinsed with an additional 20 mL of 3 mol L^{-1} HNO_3 to remove ^{243}Am. The columns were then stripped with 20 mL 1 mol L^{-1} HCl to obtain the Pu-containing fraction. Two mL of a 5 % mass fraction with water of $NaHSO_4$ was added, and the solutions were evaporated gently to dryness.

The purified Pu-containing residues were electrodeposited following an adapted procedure (Glover et al., 1998). Each residue was reconstituted with 10 mL of 0.75 mol L^{-1} H_2SO_4 and warmed on a hot plate to ensure the residue totally redissolves. Upon cooling, 5 drops thymol blue pH indicator were added, and the pH adjusted to approximately pH 2 ("salmon pink" color) with approximately 1 mL concentrated NH_4OH. The solutions were transferred to electrodeposition cells (equipped with clean stainless steel disk electrodes) with pH 2 rinse solution, and final pH adjustments after transfer were made by adding concentrated NH_4OH dropwise. The solutions were electrodeposited at 0.46 A constant current for 2 h. The stainless-steel disks (now "sources") were removed after decanting the supernatant and rinsing the cell with dilute NH_4OH, and the sources were rinsed with 80% mass fraction of ethanol and water and were then air dried. An average ^{239}Pu massic activity was found to be 0.087(1) Bq·g^{-1} where the stated uncertainty is the combined standard uncertainty, where counting statistics and within and between uncertainties of replicates were considered.

Sources were counted on the Octête PC alpha spectrometer (Ametek Ortec, Oak Ridge, TN, USA) equipped with 8 identical 450 mm^2 ion-implanted Si detectors. Spectra were obtained using Ortec Maestro acquisition software (version 7.01). Electrodeposited sources (effective source diameter = 14 mm) were measured at two different source-detector distances — 5 mm and 17 mm (Inn et al., 2008).

3.5.2. Gamma spectrometry

Analysis for photon-emitting impurities was performed using a high

Table 2
Isotopic composition results expressed as activity fractions from all methods used as measured.

Impurity Observed	Method	f_i	u/%
^{241}Am	Alpha Spectrometry	0.00162	2.2
	HPGe γ-ray spectrometry	0.0019	18
	Mass spectrometry	0.00160	0.6
	Transition edge sensor decay energy spectrometry (TES, DES)	0.00158	5.1
Combined ^{239,240}Pu	Alpha Spectrometry	0.0018	1.3
	Transition edge sensor decay energy spectrometry (TES, DES)	0.0015	8.7
^{239}Pu	Mass Spectrometry	0.001248	0.4
^{240}Pu	Mass Spectrometry	0.0003891	0.5
^{241}Pu	Mass Spectrometry	0.00160	28

purity intrinsic germanium detector: X-detector (length, $L = 36$ mm; diameter, $\phi = 43$ mm). The detector is an n-type coaxial detector with a 0.5 mm Be window. This detector and the procedures used by NIST have been described by Pibida et al. (2006, 2007). For the detection of ^{239}Np daughter impurity, the gamma-ray lines used were 209.75 keV and 334.31 keV. All gamma spectroscopy measurements were made using ampoule #1 (Fig. 1).

To obtain a reliable $f_{\mathrm{Am-241}}$, two measurements were taken. For these measurements, the Compton edge was close to the 59.54 keV gamma-ray, making it hard to distinguish the presence of ^{241}Am. The $f_{\mathrm{Am-241}}$ was found to be 0.0019 (4).

3.5.3. Mass spectrometry

Mass spectrometry was used to investigate the isotopic composition (Essex et al., 2019;Essex et al., 2023) of SRM 4332f and assess the amounts of any impurities. A single ampoule (SRM 4332f-19) was diluted with 2 % mass fraction HNO_3 to a total volume of 50 mL with the aim of obtaining a ^{243}Am mass fraction of 0.5 ng g^{-1}. The sample was measured on the Element II mass spectrometer (Thermo Fisher Scientific, Waltham, MA). The target signal intensities were for the nominal masses of $m/z = 235$, 238, 239, 240, 241, and 243. Four replicate measurements were made on the same diluted solution. The measured atom ratios were corrected for instrumental mass fractionation using the uranium isotopic standard CRM U970 (NNSA, 2020) and were corrected for instrument/analysis blank. Mass fractions were converted to isotopic activity fractions using DDEP half-lives and are shown in Table 2.

3.6. Confirmatory measurements

3.6.1. Gamma spectrometry

The ^{243}Am activity in ampoule #1 (Fig. 1) was measured five times by gamma-ray spectrometry. The lines used were 74.66 keV for ^{243}Am and 334.31 keV for the ^{239}Np. The detectors and geometries used were: T-detector (25 cm, 45 cm), X-detector (5 cm, 25 cm, 40 cm), G-detector (20 cm, 40 cm), B-detector (35 cm), R-detector (30 cm, Compton suppression). The average of the 5 measurements gave an ^{243}Am massic activity of 48.01(72) Bq·g^{-1} where the stated uncertainty is the combined standard uncertainty.

3.6.2. Live timed anticoincidence counting

Live-timed anticoincidence (LTAC) counting (Fitzgerald et al., 2015) for the ^{243}Am source was performed with a three photomultiplier tube (PMT) LS detector for the α/β channel and a NaI(Tl) detector positioned below the optical chamber for the γ/x channel. The NaI(Tl) detector has graded (Pb-Cd-Cu) shielding to reduce background counts, but was unshielded in the direction of the LS optical chamber (the vertical axis). The NaI(Tl) detector was positioned as close to the LS source as possible. Data were acquired in list mode with a CAEN desktop digitizer (DT5724) and processed with a LabVIEW script that imposes a two-PMT condition on the LS channel and allows the same data to be analyzed with variable settings for the coincidence resolving time, extendable deadtime, and the LS lower-level discriminator. Accidental coincidence rates were estimated empirically by offsetting the coincidence windows (see discussion on "chance coincidences" in Knoll, 2000). Data were corrected for background and impurities.

Anticoincidence gates were set over a low-energy region (G1: 60 keV to 170 keV), including the 106 keV ^{239}Np gamma-ray and x-rays; over a higher-energy region (G2: 170 keV to 340 keV), covering the higher-energy gamma-rays; and over a wide window (G3: 60 keV to 550 keV). Relatively high backgrounds in the NaI(Tl) channel and the low activity of the source made the measurements sensitive to the background corrections. While the count rate in G1 was highest, it was found that this gate did not allow for linear extrapolation and the departure from linearity was enough to make the extrapolated intercept very sensitive to the range of discriminator settings selected. Geant4 Monte Carlo (S. Agostinelli et al., 2003) simulations for ^{239}Np, based on the single-PMT set-up (Lucas, 1998; Fitzgerald and Schultz, 2008), reproduced this shape. The simulations were used to identify a weighted combination of G1 and G2 that would give a linear extrapolation: $Y_{\mathrm{eff}} = 0.45\ Y_1 + 0.55\ Y_2$. With the weights of the two gates being nearly equal, Y_{eff} approximates a wide open gate, akin to Y_3. The experimental data for Y_{eff} and Y_3 were extrapolated with a linear function, with fit relatively small fit residuals (<0.6 % for Y_{eff} and <0.2 % for Y_3), consistent with the fit residuals calculated with the Monte Carlo data (<0.2 %). For the final analysis, the extrapolation uncertainty was estimated from the difference between linear and quadratic extrapolations and from the Monte Carlo-predicted deviation from an intercept of 1 for ^{239}Np.

The ^{243}Am massic activity was determined to be 48.12(67) Bq·g^{-1}, where the largest contributors to the stated combined standard uncertainty were from the extrapolation and the background uncertainty.

3.6.3. Decay energy spectrometry

Measurements by Decay Energy Spectrometry (DES) using ultra-low temperature transition edge sensors (TES) (Fitzgerald et al., 2021; Carlson et al., 2024) were performed on Ampoule 2 (Fig. 1). A separate publication in these proceedings describes in detail the DES source preparation and massic activity measurements. This new method has the advantage of nearly 100 % counting efficiency for alpha decay while having energy resolution required for spectroscopically distinguishing the ^{239}Pu and ^{241}Am from the ^{243}Am, without chemical separation. In this experiment, the noise level was not low enough to quantify any ^{241}Pu in the sample. Additionally, while it was there that ^{239}Pu was present in the sample, that region of interest also contains ^{240}Pu. While an estimate and curve fit can be made for the presence of ^{240}Pu, the value for ^{239}Pu is being reported as a total $^{239,\ 240}$Pu activity.

In brief, aliquots of about 60 μg of solution (≈1.4 Bq of ^{243}Am) were deposited by a drop-on-demand inkjet device onto prepared Au foils of approximate dimensions 20 μm × 2 mm × 2 mm. The deposited solution mass was determined both by calibrating the drop mass using an ultramicrobalance and by bracketing the TES foil depositions with larger (≈300 μg) depositions into LS vials. These inkjet depositions were bracketed with pycnometer depositions (≈70 mg) into LS vials. The two batches of LS vials were measured by two commercial LS counters, the PerkinElmer Quantulus Ultra Low-Level LS Spectrometer 1220 and the PerkinElmer Tri-Carb 4910 TR I (PerkinElmer, Waltham, MA). The relative net count rates were used as a means to determine inkjet drop mass traceable to the pycnometer gravimetric measurements. After drying, the foils were folded to encompass the ^{243}Am deposit in a 4π geometry. The foils were rolled to seal and mounted on the TES sensors, which were cooled in a dilution refrigerator to a base temperature of 50 mK.

Five DES sources were measured for at least 24 h each. The spectra were compared with predictions from Geant4-based Monte Carlo simulations. The data matched the simulation for a combination of ^{243}Am, ^{241}Am, and ^{239}Pu. The simulation was further used to extrapolate the background from ^{243}Am under the ^{239}Pu spectral region of interest.

Table 3
Impurity fractions used for impurity correction. The fraction for ^{241}Am was calculated using a weighted mean and an internal and external uncertainty evaluation.

Fraction	Definition	Value	u/%
$f_{\text{Am-241}}$	Impurity fraction for ^{241}Am; $A_{\text{Am-241}}/A_{\text{Am-243}}$	0.001601	0.6
$f_{\text{Pu-239}}$	Impurity fraction for ^{239}Pu; $A_{\text{Pu-239}}/A_{\text{Am-243}}$	0.001248	0.4
$f_{\text{Pu-240}}$	Impurity fraction for ^{240}Pu; $A_{\text{Pu-240}}/A_{\text{Am-243}}$	0.0003891	0.5
$f_{\text{Pu-241}}$	Impurity fraction for ^{241}Pu; $A_{\text{Pu-241}}/A_{\text{Am-243}}$	0.00160	28

A blank foil that was processed along with the sources was also measured on multiple occasions for at least 24 h. Energy calibration was performed using γ-rays from an external ^{57}Co source. In a 65-h measurement, no events occurred with an energy above 1 MeV. The average count rate below 1 MeV was $2.87(11)\cdot10^{-3}$ s^{-1}.

The ^{243}Am activity was found to be 48.44(19) Bq·g^{-1}. The largest contributors to the stated combined standard uncertainty were from the mass (0.22 %) and source-to-source count rate standard deviation (0.19 %). The impurity fraction, $f_{\text{Pu}-239}$ was found to be $1.50(19)\cdot10^{-3}$. The $f_{\text{Am}-241}$ was found to be $1.58(8)\cdot10^{-3}$. The major uncertainties for the impurity measurements were counting statistics and, for $^{239,\ 240}$Pu, extrapolation of ^{243}Am spectrum under the ROI. The energy resolution was not adequate to fully resolve the ^{240}Pu observed by mass spectrometry from the ^{239}Pu.

The ^{239}Np activity was not quantified by DES. However, the beta spectrum qualitatively matched simulations.

4. Results and discussion

Based on the impurity measurements summarized in Table 2, weighted averages and uncertainties for f_i were adopted and applied in Equation (4) for the CNET and TDCR analyses. Table 3 gives their values used in the analyses and Table 4 gives a summary of terms.

The efficiency model based on MICELLE2 calculations and corrections for the delayed γ-transition from the 8th excited state of ^{239}Np provides a good description of the experimental CNET and TDCR data (Fig. 3), with minimal trending with efficiency (Fig. 4). The CN2003-based efficiency model, which does not include the corrections for the delayed γ-transition, shows more pronounced efficiency-dependence and results in a slightly lower calculated activity since the counting efficiency is overestimated by treating the γ-transitions from β(0,8) decays as prompt (Fig. 3).

Data acquired with the CAEN digitizer (Section 3.6.2) were processed with τ_R varying from 40 ns to 400 ns to validate the corrections to the efficiency model for the delayed γ-transition. For one source (no gray filter) and its matched blank, the change in the accidental-corrected net count rate increased by 0.47 % with the increased τ_R. Applying the efficiency model (Section 3.1) to the same data, the massic activity increased by just 0.06 %.

The massic activity that will be used for certification of the new ^{243}Am SRM is 48.42 Bq·g^{-1}, with an expanded uncertainty ($k = 2$) of 0.24 Bq·g^{-1}, with an uncertainty budget summarized in Table 5. This value is based on the CNET value and corrected for the impurities quantified in the adjacent analyses. The impurity correction changed the value of the CNET activity by 0.09 Bq·g^{-1}, which while is within the uncertainty, is an indication that previous accountings of impurities (i.e. only photon-emitting methods) were insufficient and that multiple applicable methods should be used whenever possible for future SRM production.

The TDCR and CNET uncertainty (Kossert et al., 2015) budgets are presented in Table 5. These two methods are the primary methods for the certification of the massic activity. The uncertainty budget for the TDCR measurements showed the largest dependence on within filter uncertainty, while the uncertainty for the CNET analysis had a large between-counter dependence. Both TDCR and CNET had the highest uncertainties attributed to the LS spectra model. The uncertainty due to the LS spectra model was conservatively estimated from the difference between LS efficiencies calculated with MICELLE2 and with CN2003. To make a direct comparison possible, MICELLE2 efficiency curves were generated without accounting for delayed β(0,8) decays; in this way, the principal difference between the efficiency curves was presumed to owe to the beta spectra. The average difference between the curves over the experimentally covered efficiency range was estimated as 0.2 %. The uncertainty due to the excited-state lifetime correction due to the uncertainty in the excited state half-life (4 ns) and an estimate of the coincidence timing jitter (10 ns). The commercial LS counters are more sensitive to this effect, as they have a shorter coincidence resolving time. The between-source uncertainty consisted of the quadratic combination

Table 4
Definitions of variables for correction calculations for LS measurements.

Term	Description	Source	Value
$\varepsilon_{D,8}$	Doubles counting efficiency for β decay of ^{239}Np to the 8th excited state of ^{239}Pu (β(0,8)) decays, including all subsequent β-γ cascades	Equation 1	
$\varepsilon_{D,\beta 8}$	Doubles counting efficiency for β(0,8); no relaxation from the excited state included	Equation 1	
$\varepsilon_{D,\beta\gamma 8}$	Doubles counting efficiency for β(0,8) decays assuming prompt relaxation from the 8th excited state of ^{239}Pu	Equation 1	
$\varepsilon_{D,\gamma 8}$	Doubles counting efficiency for relaxation from the 8th excited state of ^{239}Pu	Equation 1	
P_S	probability that the gamma transition from the 8th excited state of ^{239}Pu occurs within τ_R	Equation 2	
τ_R	Coincidence resolving time	Equation 2	60 ns (TDCR); 18 ns (CNET)
$T_{1/2}(\gamma)$	Half-life for the 8th excited state of ^{239}Pu	Equation 2	193 ns (DDEP)
A_m	Massic activity of ^{243}Am	Equation 3	
R_D^+	Doubles count rate for ^{243}Am, ^{239}Np, and all impurities, corrected for background and accidental coincidences	Equation 3	
ε_D^+	Doubles counting efficiency for ^{243}Am, ^{239}Np, and all impurities	Equation 3	
$\varepsilon_{D,Am\text{-}243}$	Doubles counting efficiency for ^{243}Am	Equation 4	1 per decay of ^{243}Am
$f_{\text{Np-239}}$	Impurity fraction for ^{239}Np; $A_{\text{Np-239}}/A_{\text{Am-243}}$	Equation 4	1; ^{239}Np ($T_{1/2} = 2.356(3)$ d) is in equilibrium with ^{243}Am
$f_{\text{Am-241}}$	Impurity fraction for ^{241}Am; $A_{\text{Am-241}}/A_{\text{Am-243}}$	Equation 4	See Table 3
$f_{\text{Pu-239}}$	Impurity fraction for ^{239}Pu; $A_{\text{Pu-239}}/A_{\text{Am-243}}$	Equation 4	See Table 3
$f_{\text{Pu-240}}$	Impurity fraction for ^{240}Pu; $A_{\text{Pu-240}}/A_{\text{Am-243}}$	Equation 4	See Table 3
$f_{\text{Pu-241}}$	Impurity fraction for ^{241}Pu; $A_{\text{Pu-241}}/A_{\text{Am-243}}$	Equation 4	See Table 3
$\varepsilon_{\text{Np-239}}$	Doubles counting efficiency for ^{239}Np	Equation 4	From the MICELLE2 model
$\varepsilon_{\text{Am-241}}$	Doubles counting efficiency for ^{241}Am	Equation 4	1 per decay of ^{241}Am
$\varepsilon_{\text{Pu-240}}$	Doubles counting efficiency for ^{240}Pu	Equation 4	1 per decay of ^{240}Pu
$\varepsilon_{\text{Pu-239}}$	Doubles counting efficiency for ^{239}Pu	Equation 4	1 per decay of ^{239}Pu
$\varepsilon_{\text{Pu-241}}$	Doubles counting efficiency for ^{241}Pu	Equation 4	Estimated from previous efficiency calculations

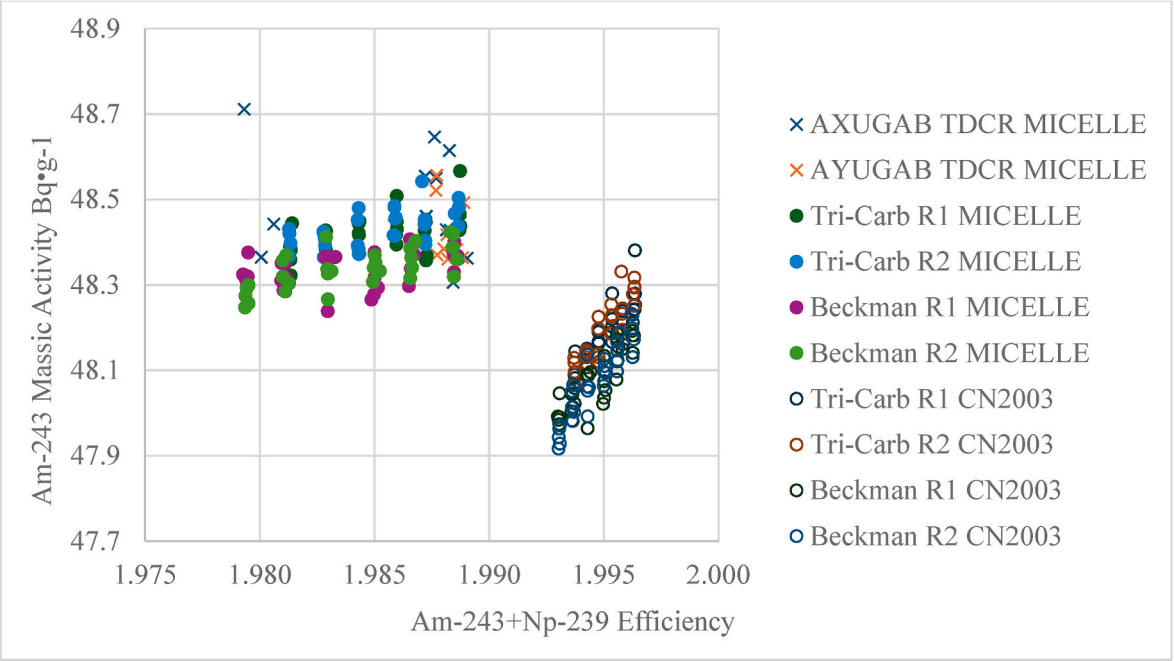

Fig. 3. TDCR (Crosses) and CNET (closed circles - MICELLE, open circles - CN2003) massic activity results. Scatter in the data at a given efficiency are repeat measurements of same source. TDCR source AXUGAB was measured with various gray filters which varied the efficiency.

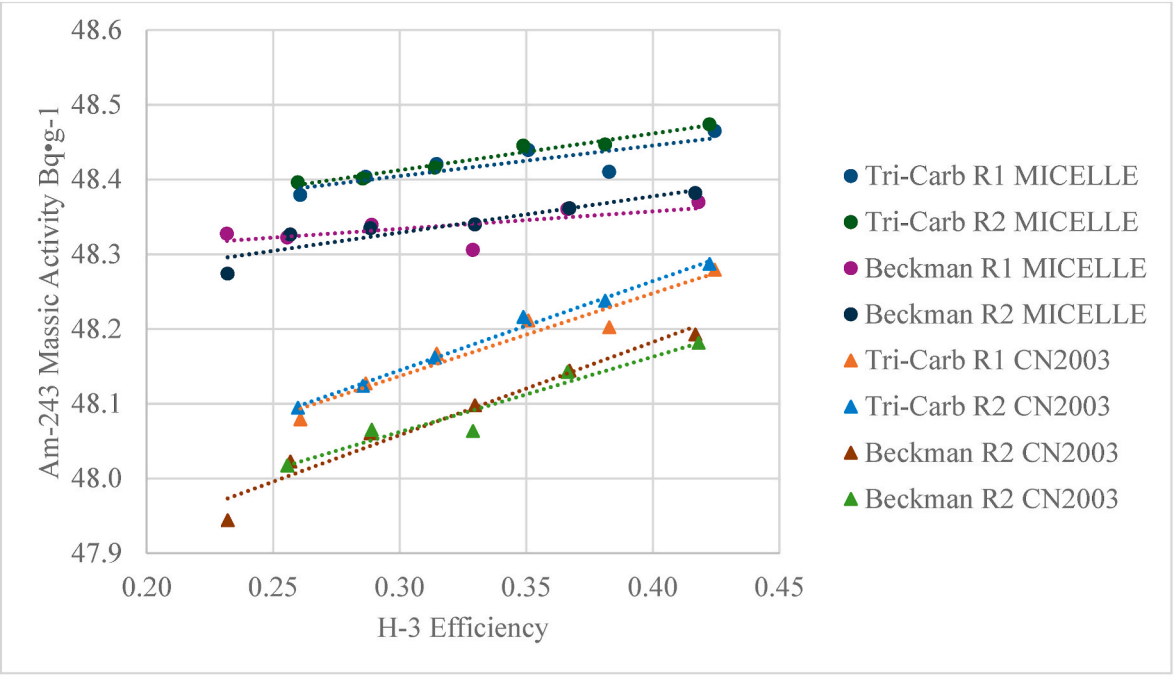

Fig. 4. The same CNET massic activity data from Fig. 3 with results averaged for each source and correlated with tritium efficiency, by code. The reduced dependence of traced activity vs tritium efficiency is evident for the MICELLE2 results.

of the full standard deviation between all sources and the percent standard deviation of the mean between cycles for each source. The within-filter uncertainty is the standard deviation of the repeat measurements of a given filter, averaged over the filters used.

5. Summary and conclusions

The standardization results for SRM 4332f were obtained from two trials, with one scintillant (UGAB), and measured in two commercial LS Counters. A tabulation of the uncertainty assessment is given in Table 5. The value of massic activity to be used for certification is 48.42(12) Bq g^{-1} of ^{243}Am and has been corrected for the impurities of ^{239}Pu, ^{240}Pu, ^{241}Pu, and ^{241}Am.

In contrast to previous issues of SRM 4332, several primary methods were used to provide confirmatory measurements. Fig. 5 shows all of the methods' activity values. Gravimetric links allowed comparisons of the current measurements to previous measurement campaigns at NIST, with activity of the previous issue being measured within its certified

Table 5
Uncertainty budgets for A) TDCR and B) CNET.

A) TDCR	u/%	B) CNET	u/%
Within Filter	0.20	Between Source	0.06
Between Filter	0.07	Birks Parameter (kB)	0.021
Between Source	0.07	^{243}Am Half-life	2.0E-06
Birks Parameter (kB)	0.011	Mass	0.05
^{243}Am Half-life	7.E−07	Background	0.0018
Mass	0.05	Impurities	0.009
Background	0.08	Excited Lifetime	0.0026
Impurities	0.012	LS spectra model	0.20
Excited Lifetime	0.0005	Wall Effect	0.025
LS spectra model	0.20	Branching Ratio	0.0097
Wall Effect	0.025	^{3}H Half-life	6.0E-06
Dilution Factor	0.00025	^{3}H Activity	0.004
Branching Ratio	0.00028	Between Counters	0.12
Combined u_c	**0.31**	Between Runs	0.007
Expanded U_c (k=2)	**0.63**	**Combined u_c**	**0.25**
		Expanded U_c (k=2)	**0.50**

uncertainty.

Confirmatory measurements for the activity showed generally good agreement. DES had a lower uncertainty than LTAC, alpha spectrometry, and gamma-ray spectrometry. The spread of activity values can be explained by some contributing factors including that few photons, low count rates, and high backgrounds increased LTAC uncertainty, and that TDCR, CNET and DES have high efficiency, good statistics, and robust analysis models.

Compared to earlier campaigns, this standardization employed a significantly improved efficiency model. Considering the 193 ns half-life of the ^{239}Pu isomeric level at 391.6 keV resulted in an appreciable change in efficiency, as the majority of gamma emissions from this level occurred outside the coincidence resolving time of the different LS counters. In earlier campaigns the impurity analysis was limited to a purely photon-based approach (HPGe gamma-ray spectrometry), while instead this analysis is sensitive to alpha and pure beta impurities by using alpha spectrometry, mass spectrometry, and DES in addition to the gamma-ray spectrometry. The complementary strengths of these methods allowed a better characterization of isobars and a much more confident impurity correction for the LS data. When considering the impact of these changes to the analyses, the efficiency models CN2003 and MICELLE2 differed by 0.87 %. CN2003 and MICELLE2 codes have very different levels of complexity, with CN2003 using stored beta shapes being much simpler but less robust, therefore this almost 1 % difference is unsurprising. The impurity correction only changed activity values by 0.19 %.

The improved efficiency model and thorough accounting for impurities resulted in a higher massic activity than determined in previous measurement campaigns and in a lower combined standard uncertainty due to reduced variability in the data due to the methods' efficiency dependence.

CRediT authorship contribution statement

M.R. Bodine: Data curation, Formal analysis, Investigation, Validation, Writing – original draft. **L. Laureano-Pérez:** Conceptualization, Funding acquisition, Investigation, Methodology, Project administration, Resources, Software, Supervision, Writing – review & editing. **R. Collé:** Conceptualization, Formal analysis, Investigation, Methodology, Resources, Supervision, Writing – review & editing. **J. Wilde:** Data curation, Formal analysis, Investigation, Software, Validation, Visualization, Writing – review & editing. **R. Fitzgerald:** Data curation, Investigation, Methodology, Software, Visualization, Writing – review & editing. **L. Pibida:** Investigation, Methodology. **J. La Rosa:** Investigation, Methodology, Resources. **A.J. Pearce:** Data curation, Formal analysis, Investigation, Resources, Writing – review & editing. **R. Essex:** Investigation, Methodology. **D.E. Bergeron:** Data curation, Investigation, Methodology, Software, Validation, Visualization, Writing – review & editing. **M. Carlson:** Data curation, Formal analysis, Investigation.

Declaration of competing interest

The authors declare the following financial interests/personal relationships which may be considered as potential competing interests: Declaring editorial roles: Given his role as Editor in Chief, Denis Bergeron had no involvement in the peer review of this article and had no access to information regarding its peer review. Full responsibility for the editorial process for this article was delegated to another journal editor.Given his role as Guest Editor, Ryan Fitzgerald had no involvement in the peer review of this article and had no access to information regarding its peer review. Full responsibility for the editorial process for this article was delegated to another journal editor. If there are other authors, they declare that they have no known competing financial

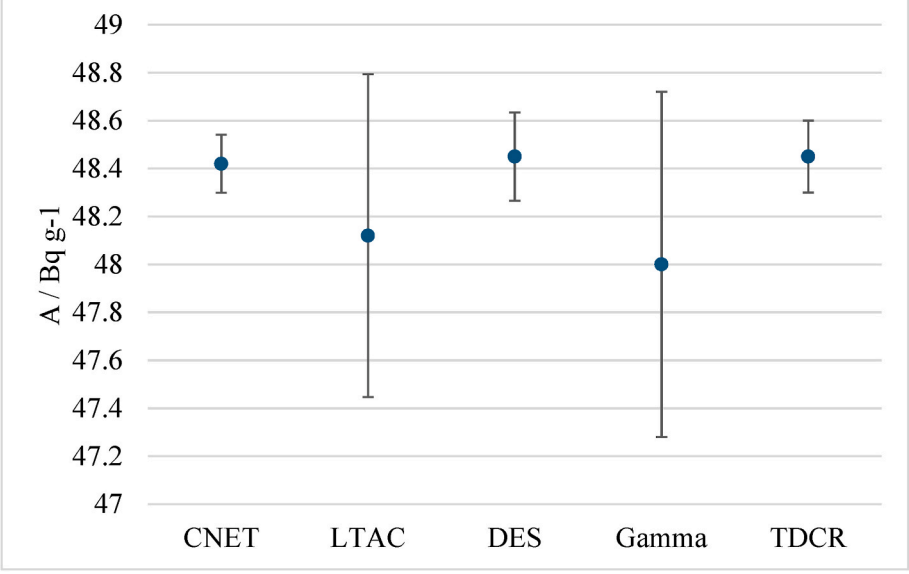

Fig. 5. A comparison of the results for the ^{243}Am massic activity. The uncertainty intervals on the data point represent the combined standard uncertainties as determined by each method.

interests or personal relationships that could have appeared to influence the work reported in this paper.

Acknowledgments

DES measurements were supported in part by NIST IMS funding.

Special thanks to Brittany Broder who performed early TDCR efficiency calculations.

We are grateful to Karsten Kossert (PTB) for many useful discussions and for providing the Pu atomic data input file for MICELLE2 calculations.

Appendix A. Supplementary data

Supplementary data to this article can be found online at https://doi.org/10.1016/j.apradiso.2026.112674.

Data availability

Data will be made available on request.

References

Agostinelli, S., Allison, J., Amako, K., Apostolakis, J., Araujo, H., Arce, P., Asai, M., Axen, D., Banerjee, S., Barrand, G., Behner, F., Bellagamba, L., Boudreau, J., Broglia, L., Brunengo, A., Burkhardt, H., Chauvie, S., Chuma, J., Chytracek, R., Zschiesche, D., 2003. Geant4—a simulation toolkit. Nucl. Instrum. Methods Phys. Res. Sect. A Accel. Spectrom. Detect. Assoc. Equip. 506 (3), 250–303. https://doi.org/10.1016/S0168-9002(03)01368-8.

Bé, M.-M., Chisté, V., Dulieu, C., Browne, E., Chechev, V., Kuzmenko, N., Kondev, F., Luca, A., Galan, M., Pearce, A., Huang, X., 2008. Monographie BIPM-5, 4. Bureau International des Poids et Mesures.

Bé, M.-M., Chisté, V., Dulieu, C., Mougeot, X., Browne, E., Chechev, V., Kuzmenko, N., Kondev, F., Luca, A., Galan, M., Nichols, A.L., Arinc, A., Huang, X., 2010. Monographie BIPM-5, 5. Bureau International des Poids et Mesures.

Barresi, A., Chiesa, D., Nastasi, M., Previtali, E., Sisti, M., 2022. High precision measurement of the half-life of the 391.6 keV metastable level in ^{239}Pu. Phys. Rev. C 105, 3. https://doi.org/10.1103/PhysRevC.105.034346.

Broda, R., Cassette, P., Kossert, K., 2007. Radionuclide metrology using liquid scintillation counting. Metrologia 44 S36. https://doi.org/10.1088/0026-1394/44/4/S06.

Campion, P.J., 1975. Procedures for Accurately Diluting and Dispensing Radioactive Solutions. Monographie BIPM-1.

Carlson, M., Fitzgerald, R., Schmidt, D., O'Neil, G., 2024. Characterization of transition edge sensors for decay energy spectrometry. J. Low Temp. Phys. 216 (1–2). https://doi.org/10.1007/s10909-024-03135-9.

Collé, R., 2019. Ampoules for Radioactivity Standard Reference Materials^{tm}. NISTIR, 8254. https://doi.org/10.6028/NIST.IR.8254.

Collé, R., Zimmerman, B.E., 1997. A compendium on the NIST radionuclidic assays of the massic activity of ^{63}Ni and ^{55}Fe Solutions Used for as Internatuonal Intercimparison of Liquid ScintillationlSpectrsmetry Techniqses. J. Res. Nat. Inst. Stand. Technol. 102 (5). https://doi.org/10.6028/jres.102.035.

Coursey, B.M., Mann, W.B., Grau Malonda, A., Garcia-Toraño, E., Los Arcos, J.M., Gibson, J.A.B., Reher, D., 1986. Standardization of carbon-14 by 4πβ liquid scintillation efficiency tracing with hydrogen-3. Int. J. Radiat. Appl. Instrum. Appl. Radiat. Isot. 37 (Issue 5), 403–408. https://doi.org/10.1016/0883-2889(86)90096-1.

Decay Data Evaluation Project, 2025. http://www.lnhb.fr/accueil/donnees-nucleaires/donnees-nucleaires-tableau/. (Accessed 6 June 2025).

Dutsov, C., Cassette, P., Sabot, B., Mitev, K., 2020. Evaluation of the accidental coincidence counting rates in TDCR counting. Nucl. Instrum. Methods Phys. Res. Sect. A Accel. Spectrom. Detect. Assoc. Equip. 977. https://doi.org/10.1016/j.nima.2020.164292.

Essex, R.M., Mann, J., Bergeron, D.E., Fitzgerald, R.P., Nour, S., Shaw, G.A., Verkouteren, R.M., 2023. Isotope dilution mass spectrometry as an independent assessment method for mass measurements of milligram quantities of aqueous solution. Int. J. Mass Spectrom. 483. https://doi.org/10.1016/j.ijms.2022.116969.

Essex, R.M., Williams, R.W., Treinen, K.C., Colle, R., Fitzgerald, R., Galea, R., Keightley, J., LaRosa, J., Laureano-Perez, L., Nour, S., Pibida, L., 2019. Preparation and calibration of a (231)Pa reference material. J. Radioanal. Nucl. Chem. 322 (3). https://doi.org/10.1007/s10967-019-06711-6.

Fitzgerald, R., Bailat, C., Bobin, C., Keightley, J., 2015. Uncertainties in 4πβ–γ coincidence counting. Metrologia 52 (3). https://doi.org/10.1088/0026-1394/52/3/S86.

Fitzgerald, R.P., et al., 2021. Toward a new primary standardization of radionuclide massic activity using microcalorimetry and quantitative milligram-scale samples, J. R. Inside NIST 126, 126048. https://doi.org/10.6028/jres.126.048.

Fitzgerald, R., Schultz, M.K., 2008. Liquid-scintillation-based anticoincidence counting of Co-60 and Pb-210. Appl. Radiat. Isot. 66 (6–7), 937–940. https://doi.org/10.1016/j.apradiso.2008.02.037.

Glover, S.E., Filby, R.H., Clark, S.B., Grytdal, S.P., 1998. Optimization and characterization of a sulfate based electrodeposition method for alpha-spectroscopy of actinide elements using chemometric analysis. J. Radioanal. Nucl. Chem. 234 (1–2), 213–220. https://doi.org/10.1007/bf02389774.

Günther, E., 2003. Personal Communication.

Inn, K.G.W., Hall, E., Woodward, J.T., Stewart, B., Pollanen, R., Selvig, L., Turner, S., Outola, I., Nour, S., Kurosaki, H., LaRosa, J., Schultz, M., Lin, Z., Yu, Z., McMahon, C., 2008. Use of thin collodion films to prevent recoil-ion contamination of alpha-spectrometry detectors. J. Radioanal. Nucl. Chem. 276 (2), 385–390. https://doi.org/10.1007/s10967-008-0516-y.

Knoll, G.F., 2000. Radiation Detection and Measurement, 3rd Ed.. Wiley. ISBN: 978-0-471-07338-3.

Kossert, K., Broda, R., Cassette, P., Ratel, G., Zimmerman, B., 2015. Uncertainty determination for activity measurements by means of the TDCR method and the CIEMAT/NIST efficiency tracing technique. Metrologia 52, S172. https://doi.org/10.1088/0026-1394/52/3/S172.

Kossert, K., Nahle, O.J., Janßen, H., 2014. Activity determination of ^{229}Th by means of liquid scintillation counting. Appl. Radiat. Isot. 87, 274–281.

Kossert, K., Grau Carles, A., 2010. Improved method for the calculation of the counting efficiency of electron-capture nuclides in liquid scintillation samples. Appl. Radiat. Isot. 68 (7–8), 1482–1488.

Laureano-Perez, L., Colle, R., Fitzgerald, R., Outola, I., Pibida, L., 2007. A liquid-scintillation-based primary standardization of ^{210}Pb. Appl. Radiat. Isot. 65 (12), 1368–1380. https://doi.org/10.1016/j.apradiso.2007.06.012.

Lucas, L.L., 1998. Calibration of the massic activity of a solution of ^{99}Tc. Appl. Radiat. Isot. 49 (9–11), 1061–1064. https://doi.org/10.1016/S0969-8043(97)10020-3.

Mougeot, X., 2017. BetaShape: a new code for improved analytical calculations of beta spectra. In: EPJ Web Conf, 12015, 146.

Mougeot, X., 2015a. Reliability of usual assumptions in the calculation of β and υ spectra. Phys. Rev. C 91, 055504.

Mougeot, X., 2015b. Erratum: reliability of usual assumptions in the calculation of β and υ spectra. Phys. Rev. C 92, 059902.

NIST, 2005. Certificate for Standard Reference Material 4334h, Plutonium 242 Radioactivity Standard. National Institute of Standards and Technology.

NIST, 2008. Certificate for Standard Reference Material 4340b, Plutonium 241 Radioactivity Standard. National Institute of Standards and Technology.

NIST, 2015. Certificate for Standard Reference Material 4927e, Tritium Radioactivity Standard. National Institute of Standards and Technology.

NIST, 2019. Certificate for Standard Reference Material 4332e, Americium Radioactivity Standard. National Institute of Standards and Technology.

NNSA, N.B.L., 2020. Certified Reference Material CRM U970, Uranium (U_3O_8) Isotopic Standard. *NBL Program Office*. U.S. Department of Energy.

Pibida, L., Hsieh, E., Fuentes-Figueroa, A., Hammond, M.M., Karam, L., 2006. Software studies for germanium detectors data analysis. Appl. Radiat. Isot. 64 (10–11), 1313–1318. https://doi.org/10.1016/j.apradiso.2006.02.076.

Pibida, L., Nafee, S.S., Unterweger, M., Hammond, M.M., Karam, L., Abbas, M.I., 2007. Calibration of HPGe gamma-ray detectors for measurement of radioactive noble gas sources. Appl. Radiat. Isot. 65 (2), 225–233. https://doi.org/10.1016/j.apradiso.2006.07.002.

Sibbens, G, Altzitzoglou, T, 2007. Preparation of radioactive sources for radionuclide metrology. Metrologia 44 (4), S71–S78. https://doi.org/10.1088/0026-1394/44/4/s09. https://iopscience.iop.org/article/10.1088/0026-1394/44/4/S09. (Accessed 2 August 2007).

Zimmerman, B.E., Colle, R., Cessna, J.T., 2004. Construction and implementation of the NIST triple-to-double coincidence ratio (TDCR) spectrometer. Appl. Radiat. Isot. 60 (2–4), 433–438. https://doi.org/10.1016/j.apradiso.2003.11.055.

Zimmerman, B.E., Colle, R., 1997. Standardization of ^{63}Ni by 4πβ Liquid Scintillation Spectrometry With ^{3}H-Standard Efficiency Tracing. J. Res. Natl. Inst. Stand. Technol. 102 (4), 455–477. https://doi.org/10.6028/jres.102.031.